Inorganic Chemistry

pubs.acs.org/IC

Article

Node-Dependent Photoinduced Electron Transfer in Third-Generation 2D MOFs Containing Earth-Abundant Metal Ions

Friedrich W. Steuber, John J. Gough, Éadaoin Whelan, Lyubomyr Burtnyak, A. Louise Bradley, and Wolfgang Schmitt*

Cite This: https://dx.doi.org/10.1021/acs.inorgchem.0c02475

Read Online

ACCESS | Metrics & More | Article Recommendations | Supporting Information

ABSTRACT: Five isostructural 2D metal−organic frameworks (MOFs), based on a photoactive Cu^{I} metallolinker and mixed mono-/dinuclear secondary building units (SBUs), are reported. The MOFs **1(M)** (M = Mn, Co, Cu, Zn, and Cd) exhibit broad absorption across the visible-light spectrum and emission centered at ca. 730 nm. Upon photoexcitation, the rigidity of the framework hinders the pseudo-Jahn−Teller distortion of the metallolinker's excited state, providing efficient intersystem crossing into the triplet state. Rapid luminescence quenching in **1(Cu)** and **1(Co)** suggests photoinduced electron transfer (PET) to the SBUs, whereas lifetimes of up to 22.2 ns are observed in **1(Zn)**. The quantum yields relative to the parent photosensitizer (PS) decrease for metal nodes containing transition metal ions with partially occupied d-orbitals but increase for the d^{10} systems Cd^{II} and Zn^{II} by a factor of up to 6. Importantly, the excited state decay rates directly correlate with the occupancy of the $[M^{II}(OH_2)]_x$ moieties in the MOFs providing nonradiative decay pathways via O−H oscillators. Cyclovoltammetry reveals minor changes in $Cu^{I/II}$ oxidation potential, with excited-state reduction potentials for **1(M)** rivalling Ru analogues. These results establish bis(diimine)copper(I) photosensitizers as viable metallolinkers for MOFs and present a rare example of an isostructural series obtained from a photosensitive metallolinker.

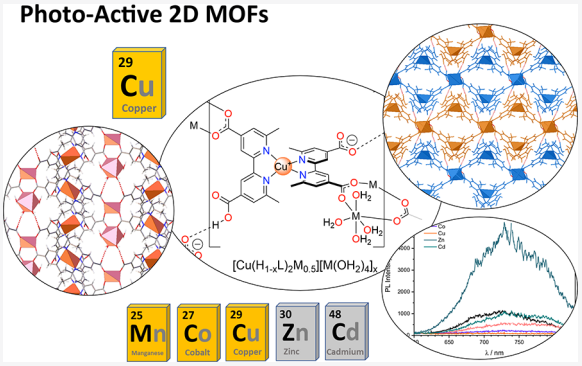

INTRODUCTION

Metal−organic frameworks (MOFs) are a novel class of materials comprising inorganic nodes, or secondary building units (SBUs), connected via organic linkers and containing potential voids.[1−3] Their tunability at a molecular level allows for the precise assembly of modulated components in a periodic environment. Thus, MOFs are outstanding candidates for applications such as gas storage, separation, sensing, catalysis, and solar energy conversion.[4,5] In the latter, notable advances have been made by moving from band gap engineering in second-generation MOFs to the incorporation of photosensitizers (PSs) with long excited-state lifetimes in third-generation MOFs.[6] This has enabled the use of metal−organic materials for sensing, photocatalysis, and artificial photosynthesis.[7−12]

With respect to the conversion of solar energy, Ru- and Ir-polypyridyl complexes in particular have been utilized as remarkable PSs and can be immobilized as guests in MOF pores or as structure-directing metallolinkers.[9,11,13−19] The latter is typically accomplished by functionalizing the polypyridyl ligands with carboxylate moieties, yet the use of Ru- and Ir-metallolinkers in practical application is stifled by their exceptionally low crustal abundance and the associated unsustainable and excessive cost requirements.

With respect to alternative PSs comprising earth-abundant metals,[20] Cu^{I} species in particular have received significant scientific attention, whereby the best performing PSs can be divided into two major groups: Diimine-diphosphine copper(I) complexes featuring metal-to-ligand charge transfer (MLCT) transitions in the (near-)visible region and luminescence that is characterized by relatively long excited-state lifetimes, some of which exhibit excited-state reduction potentials exceeding Ir-PSs.[21−23] In comparison, bis(diimine)-copper(I) complexes feature higher extinction coefficients and MLCT transitions centered in the blue region, but they generally suffer from shorter excited state lifetimes. The latter have been widely researched as dyes in dye-sensitized solar cells (DSCs), where their anchorage to nanocrystalline TiO_2 is accomplished by carboxylate/phosphonate functionalization of the ligand, providing a vast landscape of metallolinkers to be used in MOF synthesis.[24−26] A particular drawback of Cu^{I} PSs compared to Ru and Ir analogues are the lability of Cu^{I}−ligand

Received: August 19, 2020

bonds and the associated possibility of ligand exchange,[27] as well as excimer quenching of the pseudo-Jahn−Teller distorted excited state by solvents or counterions.[28,29] In this regard, their incorporation as metallolinkers in MOFs might lead to increased stability derived from the framework rigidity.

So far, the use of Cu^{I}−PSs as metallolinkers remains scarce: MOF-1040 is a triply interpenetrated analogue of the archetype MOF-5, utilising heteroleptic Cu^{I}-complexed bisdiimine [2]pseudorotaxanates as metallolinkers, in which oxidation and demetallation was accomplished while retaining the parent framework.[30] Moreover, the homoleptic Cu^{I} complex from 6,6′-dimethyl-2,2′-bipyridine-5,5′-dicarboxylic acid has been combined with La^{III} nodes to form a MOF exhibiting reversible vapor sorption.[31] However, neither of these systems have been characterized with respect to photo- and/or electrochemical properties. Recently, the UiO-type mPT-MOF (comprising mixed quarterphenyl/phenanthryl linkers and $\{Zr_6\}$ nodes) was post-synthetically modified to bear diimine-diphosphine copper(I) complexes as PSs, as well as Co/Fe- or Re-catalysts, to facilitate photocatalytic H_2 evolution and CO_2 reduction, respectively,[32,33] yet as synthetic approaches to MOFs are associated with a certain degree of serendipity, the preparation of strictly isostructural MOFs with directly comparable physicochemical properties remains challenging. Particularly, variable electronic attributes and ligand-field requirements of the elements across the fourth period of the periodic table result in significant structural variations associated with the transition metal nodes, and inherent photophysical properties of MOFs containing a specific PS are not directly comparable.[34,35]

Here, we report five new 2D MOFs **1(M)** (M = Mn, Co, Cu, Zn, and Cd) assembled from the photosensitive metallolinker $[Cu(H_2L)_2]^+$ (H_2L = 6,6′-dimethyl-2,2′-bipyridine-4,4′-dicarboxylic acid). As **1(M)** are isostructural, the system provides a unique opportunity to investigate the variation of node metals and their influence on the photophysical and electrochemical properties of the resulting framework. The reported networks exhibit broad absorption across the visible light spectrum and strong red emission whereby the framework rigidity suppresses the commonly observed pseudo-Jahn−Teller distortion of the metallolinker's excited state. Hence, the framework structure enables rapid intersystem crossing into the triplet states, whilst the nature of the transition metal node determines the photoinduced electron transfer (PET) and lifetime characteristics.

RESULTS AND DISCUSSION

As outlined in Scheme 1, **1(M)** form in good yields from 1:4 stoichiometric mixtures of *in situ* assembled $[Cu(H_2L)_2]PF_6$ and $M(NO_3)_2$ in DMF/H_2O (2:1, v/v) at 85 °C, with trifluoroacetic acid (TFA) added as a modulator. It should be noted that in the absence of water from the reaction mixture only dimethylammonium metal formates are formed,[36,37] while higher temperatures lead to the disassembly and oxidation of the thermally labile Cu^{I} complex. Variation of metal to metallolinker ratios only affects yield and crystal size but not the overall composition of the title compounds.

Scheme 1. Synthesis of 1(M) and Hydrogen Bonding Based on the Occupancy of $[M(OH_2)_4]$

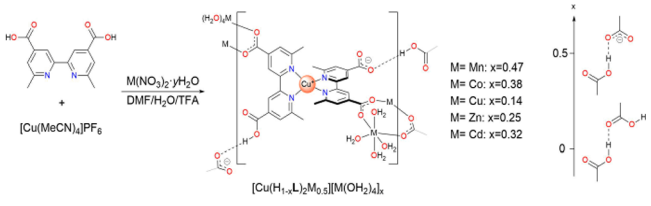

1(M) crystallize as dark red plates with yields based on the metallolinker between 34% for **1(Mn)** and 85% for **1(Zn)**. Their single-crystal structures were solved and refined in the monoclinic space group *C*2/*c* with the asymmetric units (**1(Zn)** in Figure 1, remaining **1(M)** in Figure S1), each comprising one metallolinker as well as a divalent metal ion (M = Mn, Co, Cu, Zn, and Cd) and a partially occupied tetraaquametal(II) moiety located on a two-fold symmetry axis. The coordination environment of the metallolinkers' central atom Cu1 is a distorted tetrahedron displaying virtually identical bond distances (ca. 1.99 and 2.04 Å to the pyridine moieties with uncoordinated and coordinated carboxylates per **L**, respectively) and ligand bite angles (ca. 82°) throughout the **1(M)** series (Table S3), with non-crystallographic C_2 symmetry. The dihedral angle φ around Cu1 deviates from orthogonality by 0.4° in **1(Zn)** to 2.1° in **1(Cu)**, less when compared to 2.9° observed in $[Cu(Me_2L)_2]PF_6$.[38] Methyl groups in the 6,6′-positions of H_2L provide steric shielding of Cu1, facilitating retention of its oxidation state at +1. The SBUs of **1(M)** (Figure 2) are composed of a divalent metal ion coordinated in a tetrahedral fashion (seesaw for Cu) by four carboxylate functionalities which are partially capped by a tetraaquametal(II) moiety, in which the central metal ion is coordinated in a distorted octahedral fashion. Yet, due to spatial constraints in the packing (Figure S2), i.e., overlapping tetraaquametal(II) moieties of SBUs adjacent along *b*, only one of the chemically equivalent but crystallographically distinct $[M(OH_2)_4]$ moieties can be occupied at a time. Interestingly, $[M(OH_2)_4]_x$ only occupies one potential site for **1(Mn)** and **1(Co)**, whereas they are disordered with approximate ratios of 1:1 for **1(Cu)** and **1(Zn)** and 3:1 for **1(Cd)** (Table S2).

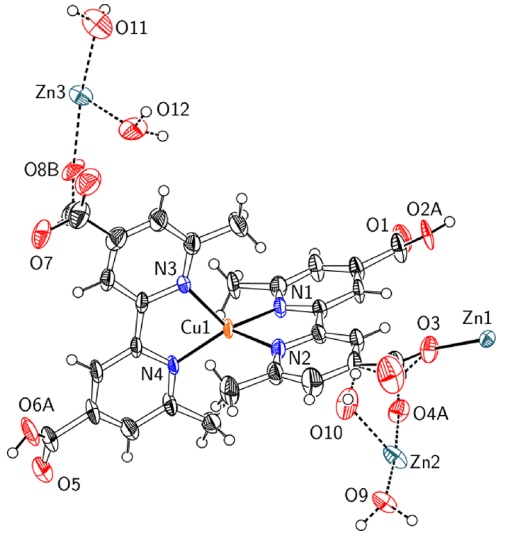

Figure 1. Thermal ellipsoid plots of the asymmetric units in the coordination polymers **1(Zn)** at 50% probability. Partially occupied moieties drawn with dashed bonds.

The two-fold connection of each Cu^{I} metallolinker to two four-connected SBUs results in corrugated 2D nets that extend

https://dx.doi.org/10.1021/acs.inorgchem.0c02475
Inorg. Chem. XXXX, XXX, XXX−XXX

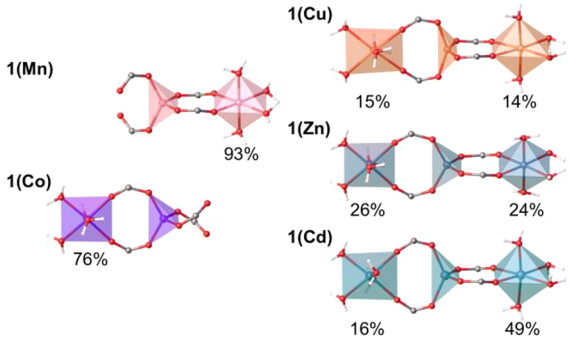

Figure 2. Coordination polyhedra of the divalent metal ions in **1(M)** and occupancies of respective $[M^{II}(OH_2)]$ moieties. Note that only up to one tetraaquametal(II) site can be occupied per SBU.

parallel to the (001) plane, which are characterized by the topological symbol **sql**. Packing diagrams of these monolayers and stacked nets are portrayed in Figure 3. Moreover, the non-coordinating carboxylate moieties of **L** exhibit varying degrees of protonation depending on the tetraaquametal(II) occupancy x (in order to achieve charge balance) and engage in strong hydrogen bonds with their equivalents that are generated through inversion symmetry. These H-bonds interconnect the 2D coordination networks, whereby the metallolinkers can be envisaged as four-connected nodes. The topology of the resulting 4,4-connected binodal 3D net gives rise to a point symbol $\{6^2.8^4\}\{6^4.8^2\}_2$. Additional hydrogen bonding involving the $[M(OH_2)_4]$ moieties leads to a 6,10-connected 3D net with the point symbol $\{3^3.4^7.5^3.6^2\}_2\{3^6.4^{14}.5^{17}.6^8\}$ (Figure S3).

The packing in **1(M)** is quite dense but features solvent pockets filled with approximately 0.75 molecules of DMF and 0.5−1 molecules of water per metallolinker. On top of the aforementioned coordination and hydrogen bonds, parallel displaced $\pi-\pi$-stacking is observed between bipyridyl moieties of adjacent layers that displays centroid-centroid distances of approximately 3.7 Å.

Powder X-ray diffraction (PXRD) reveals that **1(M)** crystallize phase pure (Figure S4). The M/Cu ratios in **1(M)** where investigated by energy-dispersive X-ray spectroscopy (EDX, Figure S7−S10) and are in accordance with the values obtained from single crystal X-ray diffraction analysis, with observed (calcd) mole ratios of 1:1 (0.96:1) for **1(Mn)**, 0.82:1 (0.88:1) for **1(Co)**, 0.71:1 (0.75:1) for **1(Zn)**, and 0.78:1 (0.82:1) for **1(Cd)**. Moreover, the Fourier-transform infrared (FTIR, Figure S5) spectra of **1(M)** are virtually identical, exhibiting differences between averaged asymmetric and symmetric carboxylate vibrations typical for bidentate bridging modes, i.e., 203 cm^{-1} (**1(Mn)**, **1(Co)**), 205 cm^{-1} (**1(Cu)**, **1(Zn)**), and 202 cm^{-1} (**1(Cd)**).[39]

$[Cu(H_2L)_2]^+$ is a well-established photosensitizer in DSCs, where it is adsorbed onto TiO_2.[24] To investigate whether it retains its optical properties upon immobilization in MOFs, solid-state photophysical studies were carried out on $[Cu(H_2L)_2]PF_6$ and crystals of **1(M)**. The absorption and emission spectra of $[Cu(H_2L)_2]PF_6$ and crystals of **1(M)**, as well as their photoluminescence decay profiles are presented in Figure 4. Solid $[Cu(H_2L)_2]PF_6$ exhibits broad absorption across the visible spectrum, and its MLCT band displays a bathochromic shift of 23−505 nm, when compared to $[Cu(H_2L)_2]Cl$ in MeOH.[40] The photophysical data demonstrates that the key attributes of $[Cu(H_2L)_2]^+$ are maintained within **1(M)**, whereby only minor differences are observed within the series of compounds. The MLCT transitions are identical with that of $[Cu(H_2L)_2]Cl$ in MeOH at 483 nm ($S_2 \leftarrow S_0$).[40,41] A second band centered at 558 nm and a shoulder showing strong absorption up to 630 nm and tapering off at 700 nm likely stem from the $S_1 \leftarrow S_0$ transition which reveals increased absorption due to reduction of symmetry.[41]

When excited at 405 nm, solid $[Cu(H_2L)_2]PF_6$ exhibits a broad emission spectrum that extends over 200 nm in the red region, peaking at 728 nm. All **1(M)** exhibit similar photoluminescence (PL) behaviour, with the exception of **1(Cu)** which is essentially non-emissive. The spectra of **1(Co)**

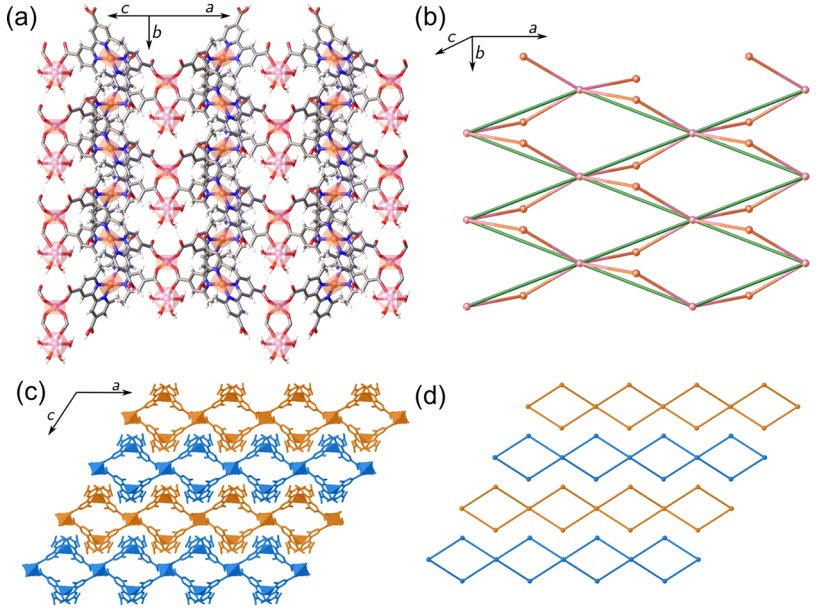

Figure 3. (a) View onto single layers in **1(Mn)** (Cu^I-based metallolinker: orange; SBUs: pink). (b) Partial and full topological reductions to a corrugated mesh wire and the underlying **sql** net (green). (c) View onto monolayers in **1(Mn)** in the direction of the crystallographic b-axis and their partial topological reduction (d).

https://dx.doi.org/10.1021/acs.inorgchem.0c02475
Inorg. Chem. XXXX, XXX, XXX−XXX

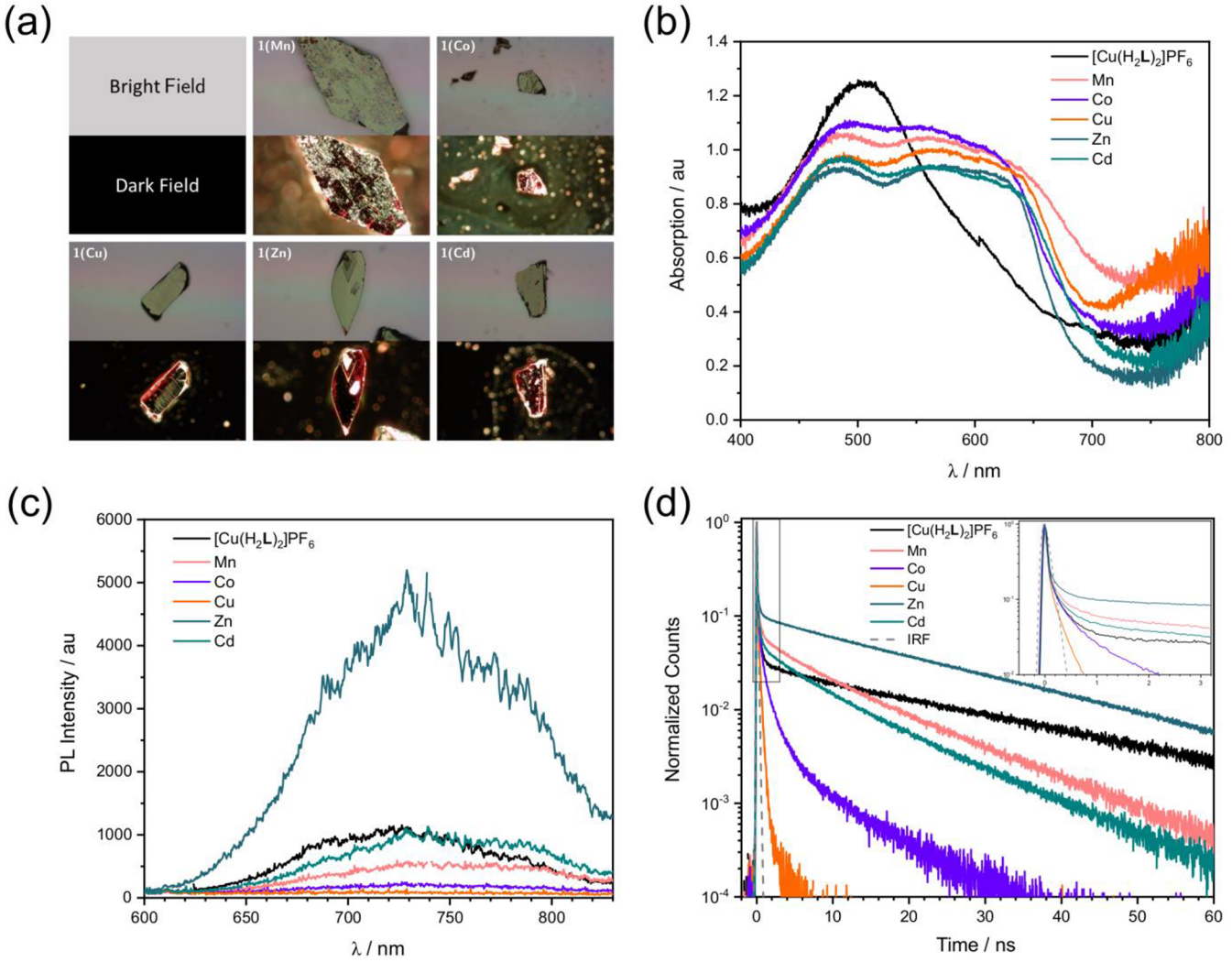

Figure 4. Bright- and dark-field images of crystals of **1(M)** used for solid-state photophysical investigations (a). Vis absorption spectra (b), steady-state emission spectra (c), and normalized photoluminescence decays (d) of $[Cu(H_2L)_2]PF_6$ and the coordination polymers **1(M)**. The inset shows the initial decay characteristics. Samples were excited at λ_{exc} = 405 nm with P_{exc} = 0.2 μW.

and **1(Zn)** are virtually identical with that of $[Cu(H_2L)_2]PF_6$, whereas **1(Mn)** and **1(Cd)** exhibit additional bands which appear as shoulders at ca. 780 nm (Figure S6). Taking into account the relative PL and relative absorption, the **1(Zn)** sample has a quantum yield (QY) almost six times that of the $[Cu(H_2L)_2]PF_6$ sample, while the relative QYs of the **1(Co)** and **1(Mn)** are respectively 0.2 and ~0.6 times that of $[Cu(H_2L)_2]PF_6$, and **1(Cd)** has a relative QY of ~1.2 (Table 1).

Time-resolved photoluminescence decays of $[Cu(H_2L)_2]$-PF_6 and **1(M)** show fast initial decays of the ^{1}MLCT states, which occur on the picosecond time scale but could not be resolved as they overlap with the instrumental response function (IRF). The residual photoluminescence associated with the ^{3}MLCT state did not decay in a mono-exponential fashion, and their average lifetimes $\langle\tau\rangle$ were extracted from a biexponential fit (see Table S4). $[Cu(H_2L)_2]PF_6$ exhibits an average lifetime of the triplet state of 26.8 ns. For **1(Cu)** and **1(Co)**, excitation of the metallolinker is followed by rapid electron transfer to the SBU, effectively quenching the photoluminescence. For the former, quenching occurs exceptionally fast so that no meaningful lifetimes could be extracted, while the latter exhibits an average lifetime of 3.0 ns. PET to the SBUs in **1(Mn)** and **1(Cd)** is stifled, leading to longer average lifetimes of 11.2 and 10.0 ns, respectively. Interestingly, the transition to the triplet state is fastest in **1(Zn)**, which exhibits an average PL lifetime of 22.2 ns. Notably, the transition from the fast-decaying singlet to the slow-decaying triplet state, i.e., intersystem crossing (ISC), occurs faster in **1(M)** when compared to the parent PS, especially for **1(Zn)**. This is due to a dependency of τ_{ISC} on the dihedral angle φ, i.e., the less φ is distorted from orthogonality (or flattens due to formal oxidation of the Cu center upon excitation), the faster the ISC occurs. This observation is in agreement with

Table 1. QYs and ^{3}MLCT-State Decay Rates of 1(M) Relative to $[Cu(H_2L)_2]PF_6$

compound	$\langle\tau\rangle$ [ns]	$\frac{QY_M}{QY_{ref}}$	$\frac{k_{r_M}}{k_{r_{ref}}}$
$[Cu(H_2L)_2]PF_6$	26.8		
1(Mn)	11.2	0.6	1.4
1(Co)	3.0	0.2	1.9
1(Zn)	22.2	5.9	7.2
1(Cd)	10.0	1.2	3.3

https://dx.doi.org/10.1021/acs.inorgchem.0c02475
Inorg. Chem. XXXX, XXX, XXX−XXX

the literature.[42] The suppression of this distortion is commonly accomplished using bulky substituents in the 2,9- and 6,6′-positions of phenanthrolines and bipyridines, respectively, which is accompanied by longer Cu−N bonds and further destabilization of the already labile complexes.[42,43] In the extended networks of **1(M)** however, the flattening distortion of the excited state is suppressed by the intrinsic framework rigidity.

The QY can also be expressed in terms of the PL decay rates, $QY = \frac{k_r}{k_r + k_{nr}}$, where k_r and k_{nr} are the radiative and nonradiative decay rates, respectively. The total decay rate, $\tau^{-1} = k_r + k_{nr}$, was estimated from the biexponential fit, as given in Table S4. Using the relative QY, the relative radiative decay rates were determined (Table 1). This is only considered for the ^{3}MLCT state, as no meaningful PL lifetime can be measured from the initial fast decay. In this case

$$\frac{k_{r_M}}{k_{r_{ref}}} = \frac{QY_M}{QY_{ref}} \times \frac{\tau_{ref}}{\tau_M}$$

where the reference refers to $[Cu(H_2L)_2]PF_6$. Interestingly, the decay rates of **1(M)** are higher compared to that of $[Cu(H_2L)_2]PF_6$ and seem to be inversely proportional to the occupancy of the $[M(OH_2)_4]$ moieties. This is counterintuitive with respect to framework rigidity, which should increase with the amount of bridging carboxylates and thus further inhibit the flattening distortion of the excited metallolinker. However, a higher $[M(OH_2)_4]$ content also provides additional pathways for nonradiative deactivation, as a result of more coordinated water molecules.[44]

Furthermore, we investigated the electrochemical behaviour of $[Cu(H_2L)_2]PF_6$ when immobilized in **1(M)** (Figure 5 and Table 2). The $Cu^{I/II}$ oxidation of $[Cu(H_2L)_2]PF_6$ is observed at 0.45 V vs. ferrocene (Fc) and is quasi-reversible, which is in accordance with reported data in MeOH.[40] Upon immobilization in the MOFs **1(M)**, the oxidation becomes electrochemically irreversible due to electron transfer limitations between the material and the electrode. If the divalent metal ion is Mn^{II} or Cd^{II}, then the oxidation potential is reduced to 0.42 V, whereas for Co^{II}, Cu^{II}, and Zn^{II} it increases by 0.06−0.11 V. The excited state reduction potential E^*_{red} can be deduced by the subtraction of the excited-state luminescence energy E_{00} from the electrochemical ground-state potential, viz. $E^*_{red} = E_{ox} - E_{00}$.[45,46] Assuming unitary charge transfer of E_{00} = 1.70 V, excited-state reduction potentials between −1.28 and −1.14 V are obtained, making **1(M)** indeed comparable to $[Ru^{II}(bpy)_3]^{2+}$-sensitized MOFs.

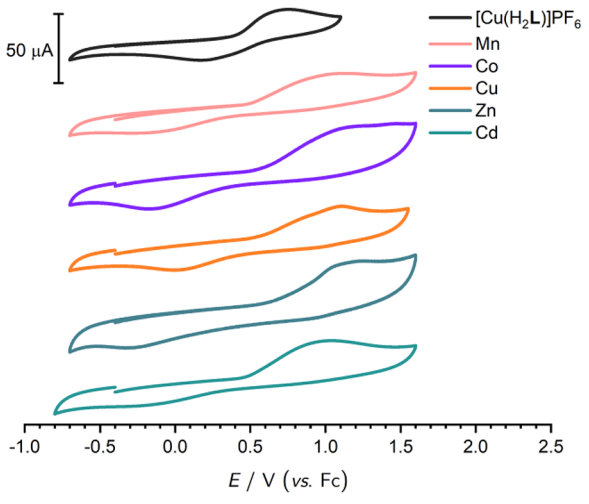

Figure 5. Cyclic voltammograms of $[Cu(H_2L)_2]PF_6$ and **1(M)**. Samples were drop-cast onto a glassy carbon electrode and fixed with Nafion ink. A 0.1 M nBu_4PF_6 MeCN solution was used as electrolyte. Scan rates were 250 mV s^{-1} (500 mV s^{-1} for **1(Zn)**).

Table 2. Oxidation (E_{ox}) and Excited State Reduction (E^*_{red}) Potentials of $[Cu(H_2L)_2]PF_6$ and 1(M) (vs $Fc^{0/+}$, in V)

	$[Cu(H_2L)_2]PF_6$	1(Mn)	1(Co)	1(Cu)	1(Zn)	1(Cd)
E_{ox}	0.45	0.42	0.51	0.56	0.53	0.42
E^*_{red}	−1.25	−1.28	−1.19	−1.14	−1.17	−1.28

CONCLUSION

In conclusion, **1(M)** represents an isostructural series of 2D MOFs assembled from a Cu^I−PS metallolinker. As a rare example of an isostructural MOF series featuring a photosensitive polypyridyl-metallolinker, **1(M)**-based MOFs grant unique insight into the variation and influence of node metals onto the photo- and electrochemical properties. Incorporation of the PS in **1(M)** leads not only to a broader absorption of visible light, but the frameworks' rigidity also allows for more efficient ISC. ^{3}MLCT lifetimes of the metallolinker are retained when coordinated to Zn^{II}, whereas fast PL quenching is observed for Co^{II} and Cu^{II}, due to photoinduced electron transfer. The QYs relative to the parent PS decrease for metal nodes featuring unpaired electrons, but they increase for Cd^{II} and up to almost six-fold for Zn^{II}. It is important to note that the excited-state decay rates correlate with the occupancy of the $[M^{II}(OH_2)]_x$ moieties in the MOFs facilitating nonradiative decay pathways via O−H oscillators. Upon incorporation into the **1(M)** frameworks, electrochemical properties of the metallolinker are largely retained, with excited-state reduction potentials being on par with those of polypyridyl-Ru analogues. Hence, these results establish Cu^I dyes as potent earth-abundant substitutes for precious metal complexes as metallolinkers for photosensitive MOFs. Future efforts are directed towards the application of **1(M)** in photocatalysis as well as the incorporation of further Cu^I dyes into earth-abundant photosensitive materials.

EXPERIMENTAL SECTION

Synthesis of $[Cu(H_{1-x}L)_2M_{0.5}][M(OH_2)_4]_x$ (1(M)). $[Cu(MeCN)_4]PF_6$ (37.27 mg, 0.1 mmol) was added to H_2L (54.45 mg, 0.2 mmol) in DMF (20 mL) resulting in a crimson solution. To an aqueous solution of $M(NO_3)_2{\cdot}yH_2O$ (0.4 mmol, 20 mL), trifluoroacetic acid (TFA, 0.8 mL), and DMF (20 mL) were added. Both solutions were combined, stirred, and divided into three 20 mL crimp vials with butyl rubber seals. The reaction mixture was heated to 80°C in a pre-heated oven for 16 h (43 h for **1(Co)**). Subsequently, the reaction mixture was cooled to room temperature, and the deep dark red crystals were filtered, washed with DMF (10 mL), H_2O (10 mL), MeOH (10 mL), and dried in air, yielding the following:

- **1(Mn)**, x = 0.47: $Mn(NO_3)_2{\cdot}4H_2O$ (100 mg). Yield: 24 mg (34%).
- **1(Co)**, x = 0.38: $Co(NO_3)_2{\cdot}6H_2O$ (116 mg). Yield: 34 mg (49%).
- **1(Cu)**, x = 0.14: $Cu(NO_3)_2{\cdot}3H_2O$ (96 mg). Yield: 40 mg (60%).
- **1(Zn)**, x = 0.25: $Zn(NO_3)_2{\cdot}6H_2O$ (119 mg). Yield: 57 mg (85%).

https://dx.doi.org/10.1021/acs.inorgchem.0c02475
Inorg. Chem. XXXX, XXX, XXX−XXX

- **1(Cd)**, x = 0.32: $Cd(NO_3)_2 \cdot 4H_2O$ (124 mg). Yield: 56 mg (76%).

For further characterizations, see Supporting Information.

■ ASSOCIATED CONTENT

Supporting Information

The Supporting Information is available free of charge at https://pubs.acs.org/doi/10.1021/acs.inorgchem.0c02475.

Materials and methods, experimental procedures, CHN analysis, FTIR spectra, SCXRD data, PXRD patterns, normalized emission spectra, luminescence lifetime calculations, SEM images and EDX spectra (PDF)

Accession Codes

CCDC 2013977−2013981 contain the supplementary crystallographic data for this paper. These data can be obtained free of charge via www.ccdc.cam.ac.uk/data_request/cif, or by emailing data_request@ccdc.cam.ac.uk, or by contacting The Cambridge Crystallographic Data Centre, 12 Union Road, Cambridge CB2 1EZ, UK; fax: +44 1223 336033.

■ AUTHOR INFORMATION

Corresponding Author

Wolfgang Schmitt − *School of Chemistry and AMBER Center, University of Dublin, Trinity College, Dublin 2, Ireland;* orcid.org/0000-0002-0058-9404; Email: schmittw@tcd.ie

Authors

Friedrich W. Steuber − *School of Chemistry and AMBER Center, University of Dublin, Trinity College, Dublin 2, Ireland*

John J. Gough − *School of Physics and AMBER Center, University of Dublin, Trinity College, Dublin 2, Ireland;* orcid.org/0000-0002-3116-2470

Éadaoin Whelan − *School of Chemistry and AMBER Center, University of Dublin, Trinity College, Dublin 2, Ireland*

Lyubomyr Burtnyak − *School of Chemistry and AMBER Center, University of Dublin, Trinity College, Dublin 2, Ireland*

A. Louise Bradley − *School of Physics and AMBER Center, University of Dublin, Trinity College, Dublin 2, Ireland;* orcid.org/0000-0002-9399-8628

Complete contact information is available at: https://pubs.acs.org/10.1021/acs.inorgchem.0c02475

Notes

The authors declare no competing financial interest.

■ ACKNOWLEDGMENTS

The authors gratefully acknowledge the Science Foundation, Ireland (13/IA/1896 and 16/IA/4550) and the European Research Council (CoG 2014-647719) for the financial support. We thank B. Twamley for many fruitful discussions regarding crystallography. Microscopy characterization and analysis has been performed at the CRANN Advanced Microscopy Laboratory.

■ REFERENCES

(1) Batten, S. R.; Champness, N. R.; Chen, X.; Garcia-Martinez, J.; Kitagawa, S.; Öhrström, L.; O'Keeffe, M.; Paik Suh, M.; Reedijk, J. Terminology of Metal−Organic Frameworks and Coordination Polymers (IUPAC Recommendations 2013). *Pure Appl. Chem.* **2013**, *85*, 1715−1724.

(2) Kitagawa, S.; Kitaura, R.; Noro, S. I. Functional Porous Coordination Polymers. *Angew. Chem., Int. Ed.* **2004**, *43*, 2334−2375.

(3) Batten, S. R.; Champness, N. R.; Chen, X.-M.; Garcia-Martinez, J.; Kitagawa, S.; Öhrström, L.; O'Keeffe, M.; Suh, M. P.; Reedijk, J. Coordination Polymers, Metal−Organic Frameworks and the Need for Terminology Guidelines. *CrystEngComm* **2012**, *14*, 3001.

(4) Lee, J.; Farha, O. K.; Roberts, J.; Scheidt, K. A.; Nguyen, S. T.; Hupp, J. T. Metal−Organic Framework Materials as Catalysts. *Chem. Soc. Rev.* **2009**, *38*, 1450.

(5) Nath, I.; Chakraborty, J.; Verpoort, F. Metal Organic Frameworks Mimicking Natural Enzymes: A Structural and Functional Analogy. *Chem. Soc. Rev.* **2016**, *45*, 4127−4170.

(6) Diercks, C. S.; Liu, Y.; Cordova, K. E.; Yaghi, O. M. The Role of Reticular Chemistry in the Design of CO2 Reduction Catalysts. *Nat. Mater.* **2018**, *17*, 301−307.

(7) Zhang, T.; Lin, W. Metal−Organic Frameworks for Artificial Photosynthesis and Photocatalysis. *Chem. Soc. Rev.* **2014**, *43*, 5982−5993.

(8) Zhu, J.; Li, P. Z.; Guo, W.; Zhao, Y.; Zou, R. Titanium-Based Metal−Organic Frameworks for Photocatalytic Applications. *Coord. Chem. Rev.* **2018**, *359*, 80−101.

(9) Lin, S.; Pineda-Galvan, Y.; Maza, W. A.; Epley, C. C.; Zhu, J.; Kessinger, M. C.; Pushkar, Y.; Morris, A. J. Electrochemical Water Oxidation by a Catalyst-Modified Metal−Organic Framework Thin Film. *ChemSusChem* **2017**, *10*, 514−522.

(10) Maza, W. A.; Haring, A. J.; Ahrenholtz, S. R.; Epley, C. C.; Lin, S. Y.; Morris, A. J. Ruthenium(II)-Polypyridyl Zirconium(IV) Metal−Organic Frameworks as a New Class of Sensitized Solar Cells. *Chem. Sci.* **2016**, *7*, 719−727.

(11) Maza, W. A.; Padilla, R.; Morris, A. J. Concentration Dependent Dimensionality of Resonance Energy Transfer in a Postsynthetically Doped Morphologically Homologous Analogue of UiO-67 MOF with a Ruthenium(II) Polypyridyl Complex. *J. Am. Chem. Soc.* **2015**, *137*, 8161−8168.

(12) Dolgopolova, E. A.; Rice, A. M.; Martin, C. R.; Shustova, N. B. Photochemistry and Photophysics of MOFs: Steps towards MOF-Based Sensing Enhancements. *Chem. Soc. Rev.* **2018**, *47*, 4710−4728.

(13) Thompson, D. W.; Ito, A.; Meyer, T. J. [Ru(Bpy)3]2+* and Other Remarkable Metal-to-Ligand Charge Transfer (MLCT) Excited States. *Pure Appl. Chem.* **2013**, *85*, 1257−1305.

(14) Martins, L.; Macreadie, L. K.; Sensharma, D.; Vaesen, S.; Zhang, X.; Gough, J. J.; O'Doherty, M.; Zhu, N.-Y.; Rüther, M.; O'Brien, J. E.; Bradley, A. L.; Schmitt, W. Light-Harvesting, 3rd Generation Ru II /Co II MOF with a Large, Tubular Channel Aperture. *Chem. Commun.* **2019**, *55*, 5013−5016.

(15) Zhang, S.; Li, L.; Zhao, S.; Sun, Z.; Luo, J. Construction of Interpenetrated Ruthenium Metal-Organic Frameworks as Stable Photocatalysts for CO2 Reduction. *Inorg. Chem.* **2015**, *54*, 8375−8379.

(16) Wang, C.; Xie, Z.; Dekrafft, K. E.; Lin, W. Doping Metal-Organic Frameworks for Water Oxidation, Carbon Dioxide Reduction, and Organic Photocatalysis. *J. Am. Chem. Soc.* **2011**, *133*, 13445−13454.

(17) Yan, Z. H.; Du, M. H.; Liu, J.; Jin, S.; Wang, C.; Zhuang, G. L.; Kong, X. J.; Long, L. S.; Zheng, L. S. Photo-Generated Dinuclear {Eu(II)}2 Active Sites for Selective CO2 Reduction in a Photosensitizing Metal-Organic Framework. *Nat. Commun.* **2018**, *9*, 1−9.

(18) Dhakshinamoorthy, A.; Asiri, A. M.; García, H. Metal-Organic Framework (MOF) Compounds: Photocatalysts for Redox Reactions and Solar Fuel Production. *Angew. Chem., Int. Ed.* **2016**, *55*, 5414−5445.

(19) Wang, C.; Dekrafft, K. E.; Lin, W. Pt Nanoparticles@ photoactive Metal-Organic Frameworks: Efficient Hydrogen Evolution via Synergistic Photoexcitation and Electron Injection. *J. Am. Chem. Soc.* **2012**, *134*, 7211−7214.

(20) Wenger, O. S. Photoactive Complexes with Earth-Abundant Metals. *J. Am. Chem. Soc.* **2018**, *140*, 13522−13533.

(21) Zhang, Y.; Schulz, M.; Wächtler, M.; Karnahl, M.; Dietzek, B. Heteroleptic Diimine−Diphosphine Cu(I) Complexes as an Alternative towards Noble-Metal Based Photosensitizers: Design Strategies, Photophysical Properties and Perspective Applications. *Coord. Chem. Rev.* **2018**, *356*, 127−146.
(22) Czerwieniec, R.; Leitl, M. J.; Homeier, H. H. H.; Yersin, H. Cu(I) Complexes − Thermally Activated Delayed Fluorescence. Photophysical Approach and Material Design. *Coord. Chem. Rev.* **2016**, *325*, 2−28.
(23) Hockin, B. M.; Li, C.; Robertson, N.; Zysman-Colman, E. Photoredox Catalysts Based on Earth-Abundant Metal Complexes. *Catal. Sci. Technol.* **2019**, *9*, 889−915.
(24) Housecroft, C. E.; Constable, E. C. The Emergence of Copper(I)-Based Dye Sensitized Solar Cells. *Chem. Soc. Rev.* **2015**, *44*, 8386−8398.
(25) Bozic-Weber, B.; Constable, E. C.; Housecroft, C. E. Light Harvesting with Earth Abundant D-Block Metals: Development of Sensitizers in Dye-Sensitized Solar Cells (DSCs). *Coord. Chem. Rev.* **2013**, *257*, 3089−3106.
(26) Magni, M.; Biagini, P.; Colombo, A.; Dragonetti, C.; Roberto, D.; Valore, A. Versatile Copper Complexes as a Convenient Springboard for Both Dyes and Redox Mediators in Dye Sensitized Solar Cells. *Coord. Chem. Rev.* **2016**, *322*, 69−93.
(27) Ward, R. Photochemistry and Photophysics of Coordination Compounds, Parts I & II. *Platinum Met. Rev.* **2009**, *53*, 45−47.
(28) Cunningham, C. T.; Moore, J. J.; Cunningham, K. L. H.; Fanwick, P. E.; McMillin, D. R. Structural and Photophysical Studies of Cu(NN)2+ Systems in the Solid State. Emission at Last from Complexes with Simple 1,10-Phenanthroline Ligands. *Inorg. Chem.* **2000**, *39*, 3638−3644.
(29) Iwamura, M.; Takeuchi, S.; Tahara, T. Real-Time Observation of the Photoinduced Structural Change of Bis(2,9-Dimethyl-1,10-Phenanthroline)Copper(I) by Femtosecond Fluorescence Spectroscopy: A Realistic Potential Curve of the Jahn-Teller Distortion. *J. Am. Chem. Soc.* **2007**, *129*, 5248−5256.
(30) Coskun, A.; Hmadeh, M.; Barin, G.; Gándara, F.; Li, Q.; Choi, E.; Strutt, N. L.; Cordes, D. B.; Slawin, A. M. Z.; Stoddart, J. F.; Sauvage, J.-P.; Yaghi, O. M. Metal-Organic Frameworks Incorporating Copper-Complexed Rotaxanes. *Angew. Chem., Int. Ed.* **2012**, *51*, 2160−2163.
(31) Kobayashi, A.; Sugiyama, A.; Ohba, T.; Suzuki, Y.; Chang, H.-C.; Kato, M. Synthesis and Vapor-Adsorption Behavior of a Flexible Porous Coordination Polymer Built from a Bis(Bipyridyl)−Cu(I) Metalloligand. *Chem. Lett.* **2014**, *43*, 1070−1072.
(32) Feng, X.; Pi, Y.; Song, Y.; Brzezinski, C.; Xu, Z.; Li, Z.; Lin, W. Metal−Organic Frameworks Significantly Enhance Photocatalytic Hydrogen Evolution and CO_2 Reduction with Earth-Abundant Copper Photosensitizers. *J. Am. Chem. Soc.* **2020**, *142*, 690−695.
(33) Pi, Y.; Feng, X.; Song, Y.; Xu, Z.; Li, Z.; Lin, W. Metal−Organic Frameworks Integrate Cu Photosensitizers and Secondary Building Unit-Supported Fe Catalysts for Photocatalytic Hydrogen Evolution. *J. Am. Chem. Soc.* **2020**, *142*, 10302.
(34) Kobayashi, A.; Ohba, T.; Saitoh, E.; Suzuki, Y.; Noro, S.; Chang, H.-C.; Kato, M. Flexible Coordination Polymers Composed of Luminescent Ruthenium(II) Metalloligands: Importance of the Position of the Coordination Site in Metalloligands. *Inorg. Chem.* **2014**, *53*, 2910−2921.
(35) Huo, D.; Lin, F.; Chen, S.; Ni, Y.; Wang, R.; Chen, H.; Duan, L.; Ji, Y.; Zhou, A.; Tong, L. Ruthenium Complex-Incorporated Two-Dimensional Metal−Organic Frameworks for Cocatalyst-Free Photocatalytic Proton Reduction from Water. *Inorg. Chem.* **2020**, *59*, 2379−2386.
(36) Jain, P.; Dalal, N. S.; Toby, B. H.; Kroto, H. W.; Cheetham, A. K. Order−Disorder Antiferroelectric Phase Transition in a Hybrid Inorganic−Organic Framework with the Perovskite Architecture. *J. Am. Chem. Soc.* **2008**, *130*, 10450−10451.
(37) Jain, P.; Ramachandran, V.; Clark, R. J.; Zhou, H. D.; Toby, B. H.; Dalal, N. S.; Kroto, H. W.; Cheetham, A. K. Multiferroic Behavior Associated with an Order-Disorder Hydrogen Bonding Transition in Metal-Organic Frameworks (MOFs) with the Perovskite ABX 3 Architecture. *J. Am. Chem. Soc.* **2009**, *131*, 13625−13627.
(38) Bessho, T.; Constable, E. C.; Graetzel, M.; Hernandez Redondo, A.; Housecroft, C. E.; Kylberg, W.; Nazeeruddin, M. K.; Neuburger, M.; Schaffner, S. An Element of Surprise—Efficient Copper-Functionalized Dye-Sensitized Solar Cells. *Chem. Commun.* **2008**, No. 32, 3717.
(39) Deacon, G. B. Relationships between the Carbon-Oxygen Stretching Frequencies of Carboxylato Complexes and the Type of Carboxylate Coordination. *Coord. Chem. Rev.* **1980**, *33*, 227−250.
(40) Constable, E. C.; Redondo, A. H.; Housecroft, C. E.; Neuburger, M.; Schaffner, S. Copper(I) Complexes of 6,6′-Disubstituted 2,2′-Bipyridine Dicarboxylic Acids: New Complexes for Incorporation into Copper-Based Dye Sensitized Solar Cells (DSCs). *Dalt. Trans.* **2009**, No. 33, 6634.
(41) Iwamura, M.; Takeuchi, S.; Tahara, T. Ultrafast Excited-State Dynamics of Copper(I) Complexes. *Acc. Chem. Res.* **2015**, *48*, 782−791.
(42) Gothard, N. A.; Mara, M. W.; Huang, J.; Szarko, J. M.; Rolczynski, B.; Lockard, J. V.; Chen, L. X. Strong Steric Hindrance Effect on Excited State Structural Dynamics of Cu(I) Diimine Complexes. *J. Phys. Chem. A* **2012**, *116*, 1984−1992.
(43) McCusker, C. E.; Castellano, F. N. Design of a Long-Lifetime, Earth-Abundant, Aqueous Compatible Cu(I) Photosensitizer Using Cooperative Steric Effects. *Inorg. Chem.* **2013**, *52*, 8114−8120.
(44) Kobayashi, A.; Arata, R.; Ogawa, T.; Yoshida, M.; Kato, M. Effect of Water Coordination on Luminescent Properties of Pyrazine-Bridged Dinuclear Cu(I) Complexes. *Inorg. Chem.* **2017**, *56*, 4280−4288.
(45) Meyer, T. J. Photochemistry of Metal Coordination Complexes: Metal to Ligand Charge Transfer Excited States. *Pure Appl. Chem.* **1986**, *58*, 1193−1206.
(46) Juris, A.; Balzani, V.; Barigelletti, F.; Campagna, S.; Belser, P.; von Zelewsky, A. Ru(II) Polypyridine Complexes: Photophysics, Photochemistry, Eletrochemistry, and Chemiluminescence. *Coord. Chem. Rev.* **1988**, *84*, 85−277.

https://dx.doi.org/10.1021/acs.inorgchem.0c02475
Inorg. Chem. XXXX, XXX, XXX−XXX